Case Western Reserve University

Scholarly Commons @ Case Western Reserve University

Scholarly Commons @ Case Western Reserve University

Faculty Scholarship

9-28-2016

Heteroepitaxy of N-type β-Ga2O3 Thin Films on Sapphire Substrate by Low Pressure Chemical Vapor Deposition

Subrina Rafique
Case Western Reserve University

Lu Han
Case Western Reserve University

Roger H. French
Case Western Reserve University, roger.french@case.edu

Hongping Zhao
Case Western Reserve University

Author(s) ORCID Identifier:

Roger H. French

Follow this and additional works at: https://commons.case.edu/facultyworks

Recommended Citation
Rafique, Subrina; Han, Lu; French, Roger H.; and Zhao, Hongping, "Heteroepitaxy of N-type β-Ga2O3 Thin Films on Sapphire Substrate by Low Pressure Chemical Vapor Deposition" (2016). *Faculty Scholarship*. 74.
https://commons.case.edu/facultyworks/74

This Article is brought to you for free and open access by Scholarly Commons @ Case Western Reserve University. It has been accepted for inclusion in Faculty Scholarship by an authorized administrator of Scholarly Commons @ Case Western Reserve University. For more information, please contact digitalcommons@case.edu.

CWRU authors have made this work freely available. Please tell us how this access has benefited or impacted you!

Applied Physics Letters

Heteroepitaxy of N-type β-Ga_2O_3 thin films on sapphire substrate by low pressure chemical vapor deposition

Cite as: Appl. Phys. Lett. **109**, 132103 (2016); https://doi.org/10.1063/1.4963820
Submitted: 01 August 2016 • Accepted: 19 September 2016 • Published Online: 28 September 2016

Subrina Rafique, Lu Han, Adam T. Neal, et al.

COLLECTIONS

Paper published as part of the special topic on The Dawn of Gallium Oxide Microelectronics

View Online

Export Citation

CrossMark

ARTICLES YOU MAY BE INTERESTED IN

A review of Ga_2O_3 materials, processing, and devices
Applied Physics Reviews **5**, 011301 (2018); https://doi.org/10.1063/1.5006941

Homoepitaxial growth of β-Ga_2O_3 thin films by low pressure chemical vapor deposition
Applied Physics Letters **108**, 182105 (2016); https://doi.org/10.1063/1.4948944

Gallium oxide (Ga_2O_3) metal-semiconductor field-effect transistors on single-crystal β-Ga_2O_3 (010) substrates
Applied Physics Letters **100**, 013504 (2012); https://doi.org/10.1063/1.3674287

Characterizing nanostructures?
Learn about a new way to get high-quality data in a fraction of the time
Read the tech note
Lake Shore CRYOTRONICS

AIP Publishing

© 2016 Author(s).

Heteroepitaxy of N-type β-Ga_2O_3 thin films on sapphire substrate by low pressure chemical vapor deposition

Subrina Rafique,[1] Lu Han,[1] Adam T. Neal,[2,3] Shin Mou,[2] Marko J. Tadjer,[4] Roger H. French,[5] and Hongping Zhao[1,a)]

[1]*Department of Electrical Engineering and Computer Science, Case Western Reserve University, Cleveland, Ohio 44106, USA*
[2]*Air Force Research Laboratory, Materials and Manufacturing Directorate, Wright-Patterson Air Force Base, Ohio 45433, USA*
[3]*Universal Technology Corporation, Dayton, Ohio 45432, USA*
[4]*United States Naval Research Laboratory, Washington, DC 20375, USA*
[5]*Department of Materials Science and Engineering, Case Western Reserve University, Cleveland, Ohio 44106, USA*

(Received 1 August 2016; accepted 19 September 2016; published online 28 September 2016)

This paper presents the heteroepitaxial growth of ultrawide bandgap β-Ga_2O_3 thin films on c-plane sapphire substrates by low pressure chemical vapor deposition. N-type conductivity in silicon (Si)-doped β-Ga_2O_3 films grown on sapphire substrate is demonstrated. The thin films were synthesized using high purity metallic gallium (Ga) and oxygen (O_2) as precursors. The morphology, crystal quality, and properties of the as-grown thin films were characterized and analyzed by field emission scanning electron microscopy, X-ray diffraction, electron backscatter diffraction, photoluminescence and optical, photoluminescence excitation spectroscopy, and temperature dependent van der Pauw/Hall measurement. The optical bandgap is ~4.76 eV, and room temperature electron mobility of 42.35 cm^2/V s was measured for a Si-doped heteroepitaxial β-Ga_2O_3 film with a doping concentration of 1.32×10^{18} cm^{-3}. *Published by AIP Publishing.* [http://dx.doi.org/10.1063/1.4963820]

Ultrawide bandgap (UWBG) gallium oxide (Ga_2O_3) is an emerging semiconductor material that has a bandgap of ~4.5–4.9 eV and is the second widest after diamond (~5.5 eV) and much higher than GaN (~3.4 eV) and 4H-SiC (~3.2 eV).[1] The critical electric field for Ga_2O_3 is estimated to be 8 MV/cm based on the empirical relationship between bandgap and breakdown field.[1] Ga_2O_3 exhibits high transparency in the deep ultraviolet (UV) and visible wavelength region due to its very large bandgap and has a transmittance of over 80% in the UV region. These unique properties make Ga_2O_3 a promising candidate for high power electronic devices and solar blind photodetectors. More importantly, bulk Ga_2O_3 for use as substrates can be grown by low cost and scalable melting growth techniques such as edge-defined film-fed growth (EFG),[2,3] floating zone (FZ)[4–6] and Czochralski[7–9] methods. β-Ga_2O_3 ingots and 2-in.-diameter β-Ga_2O_3 wafers are commercially available from Tamura Inc. (Japan).

Essential requirements for device quality epitaxial thin films are a high degree of purity, crystallinity, controllable doping, all achieved with reasonable growth rates. Current efforts for Ga_2O_3 thin film synthesis have mainly focused on the homoepitaxy in the available commercial Ga_2O_3 substrates.[10–15] While the traditional molecular beam epitaxy (MBE) growth method can produce high quality Ga_2O_3 materials, the challenge of slow growth rates still need to be addressed.[11,12] Among the limited efforts towards heteroepitaxy of β-Ga_2O_3 thin films on foreign substrates,[16–32] none has reported heteroepitaxial Ga_2O_3 films with good electrical properties.

Previously, we have demonstrated the feasibility to synthesize β-Ga_2O_3 on sapphire substrates via low pressure chemical vapor deposition (LPCVD),[26] as well as the LPCVD synthesis of high quality β-Ga_2O_3 homoepitaxial films on (010) β-Ga_2O_3 substrates.[33] In addition, we also demonstrated the synthesis of β-Ga_2O_3 rod structures on 3C-SiC-on-Si substrates via LPCVD.[34]

In this letter, we used optimized LPCVD process to synthesize high electrical quality β-Ga_2O_3 heteroepitaxial thin films grown on c-plane sapphire substrates. N-type doping of the heteroepitaxial β-Ga_2O_3 thin films with Si dopant was demonstrated in this study, which has not been reported previously. Si doping of β-Ga_2O_3 bulk crystals by FZ technique has been reported.[35] The reported Si doping concentration ranges between 10^{16} and 10^{18} cm^{-3} with a mobility of ~100 cm^2/V s. The recent report of metalorganic vapor phase epitaxy (MOVPE) growth of n-type β-Ga_2O_3 thin films on sapphire substrates did not show electrical conductivity even after Si species activation annealing.[36] Such phenomenon was attributed to the formation of SiO_2 and compensation of Si donors by Ga vacancies. The electrical conductivity of the Si-doped β-Ga_2O_3 thin films reported in this paper indicates the growth method via LPCVD is a feasible approach to grow high quality β-Ga_2O_3 thin films. The thin film morphology, crystal structure, optical and electrical properties of the as-grown n-doped β-Ga_2O_3 were characterized systematically.

C-plane sapphire substrates were used as the growth substrates, which were cleaned with acetone and isopropanol, rinsed by de-ionized water and dried with nitrogen flow

a)Author to whom correspondence should be addressed. Electronic mail: hongping.zhao@case.edu

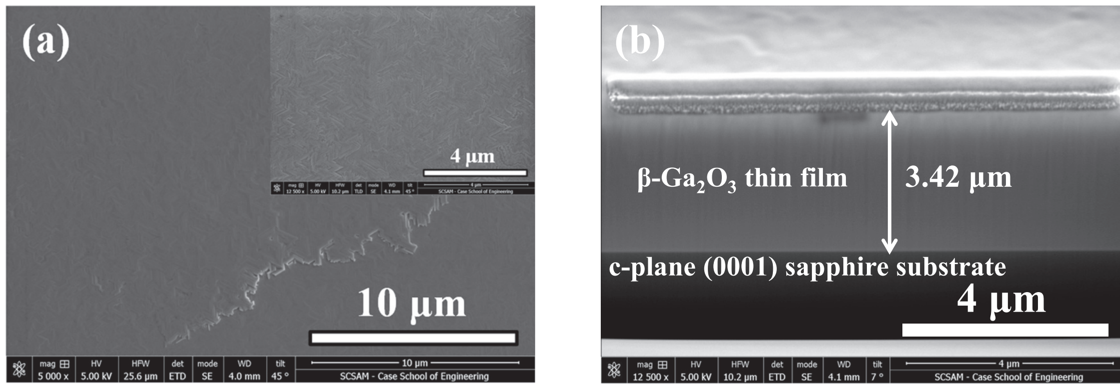

FIG. 1. (a) Top view FESEM image of as-grown UID β-Ga_2O_3 thin film grown on c-plane sapphire substrate. Inset shows the high magnification top view of the FESEM image. (b) Cross sectional FESEM image of UID β-Ga_2O_3 thin film. Layer thickness is $\sim$3.42 μm.

before growth. High purity gallium pellets (Alfa Aesar, 99.99999%) and oxygen (O_2) gas were used as the precursors for gallium and oxygen, respectively. Argon (Ar) was used as the carrier gas. The LPCVD growths of β-Ga_2O_3 on sapphire were optimized by tuning the growth temperatures, growth pressure, and oxygen volume percentages. $SiCl_4$ was used as an n-type dopant gas.

The structure, crystal quality, optical, and electrical properties of the heteroepitaxial β-Ga_2O_3 thin films were characterized by using field emission scanning electron microscopy (FESEM), X-ray diffraction (XRD), electron backscatter diffraction (EBSD), photoluminescence (PL), and photoluminescence excitation (PLE) spectroscopy, and van der Pauw/Hall measurement. The FESEM images were taken with Helios 650. XRD spectrum was collected on a Rigaku Ultima IV X-Ray Diffractometer with Cu Kα radiation (1.54 Å). Pole figure measurements were performed with Nova Nanolab 200. The absorbance measurement was characterized by using Cary 6000i UV-VIS-NIR spectrophotometer in the spectral range from 180 nm to 1800 nm with an incidence angle of 8°. PL and PLE spectra were measured using a Jobin Yvon-spex-Fluorog-3-Spectrofluorimeter. The carrier concentration and electron Hall mobility were measured with HMS 3000 Hall measurement system. Temperature dependent Hall measurement was carried out using two custom built systems. Below room temperature, an electromagnet with a vacuum cryostat with closed-cycle He refrigerator was used. Above room temperature, an electromagnet with a quartz tube and silicon carbide heater was used. Nitrogen gas was used to purge the quartz tube during high temperature measurements.

Figure 1(a) shows the top view FESEM image of a heteroepitaxial unintentionally doped (UID) β-Ga_2O_3 thin film grown for 2 h on a c-plane sapphire substrate at 800 °C. The thin film is composed of small domains having pseudo hexagonal morphology. The cross-sectional FESEM image [Fig. 1(b)] of the β-Ga_2O_3 thin film was obtained from the same sample, which shows the film thickness of 3.42 μm. This corresponds to a growth rate of $\sim$1.7 μm/h for this film. Due to the relatively fast growth rate, we observe the film surface is relatively rough, which is similar to those grown via halide vapor phase epitaxy (HVPE).[15] By tuning the growth parameters, we were able to achieve growth rates up to 6 μm/h for both UID and Si-doped β-Ga_2O_3 thin films. The surface morphology gets rougher as the film growth rate increases. The Si-doped β-Ga_2O_3 thin films have similar growth rates and surface morphology as those of UID ones grown at a similar growth condition.

The crystal quality of the doped β-Ga_2O_3 thin films grown at 900 °C was characterized by XRD and rocking curve measurement. Figure 2(a) shows the XRD θ-2θ scan spectrum of the Si-doped β-Ga_2O_3 thin film having a doping concentration of 7.57×10^{18} cm^{-3}. The three dominant peaks correspond to the ($-$201) and higher order diffraction peaks of β-Ga_2O_3, indicating that the as-synthesized thin film is phase pure with [$-$201] as the growth orientation. This is because the oxygen atoms of (0001) plane of sapphire substrate have a similar atomic arrangement as the ($-$201)

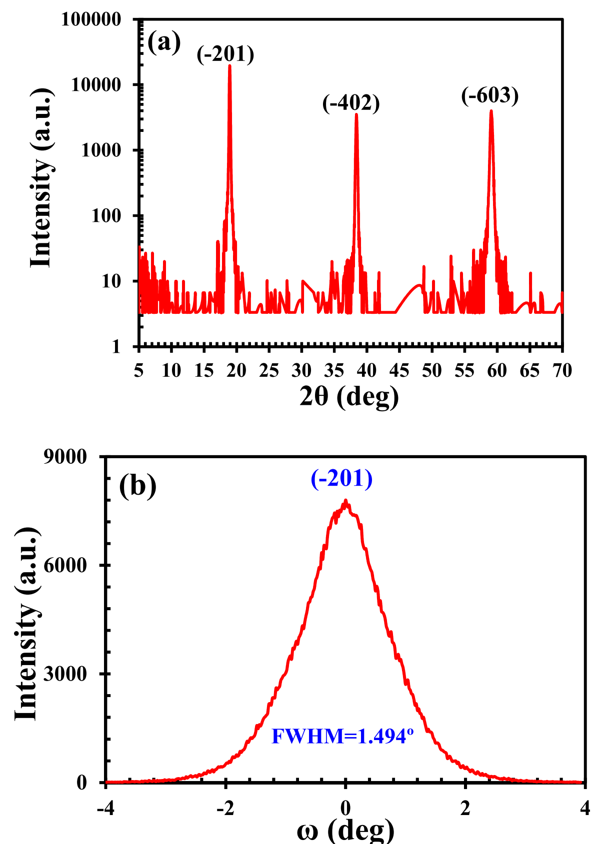

FIG. 2. (a) XRD spectrum (θ–2θ scan) of Si-doped β-Ga_2O_3 thin film. (b) XRD rocking curve of ($-$201) reflection of Si-doped β-Ga_2O_3 thin film.

equivalent plane of β-Ga_2O_3.[37] Figure 2(b) shows the XRD rocking curve of the (−201) diffraction peak of the same Si-doped β-Ga_2O_3 thin film. The full width at half maximum (FWHM) of the rocking curve is measured as 1.494°. The FWHM of the (−201) diffraction peak for the UID and Si-doped β-Ga_2O_3 thin films were similar indicating no significant crystal quality degradation due to doping. As a comparison, the reported representative FWHMs of heteroepitaxial β-Ga_2O_3 thin films grown on c-plane sapphire substrates are 0.9° (MBE, (−201) diffraction peak),[18] 0.6° (metal organic chemical vapor deposition (MOCVD), (−201) diffraction peak),[23] and 2.42° (MOVPE, (−402) diffraction peak).[38]

To study the crystallographic texture of the β-Ga_2O_3 thin film, EBSD pole figures were measured as shown in Fig. 3. The measurement was taken over a surface area of $10 \times 10\,\mu m^2$. The sharp clusters of the poles indicate high texture quality of the grown film. Results confirmed that (−201) the plane of β-Ga_2O_3 is parallel to the surface of c-plane (0001) sapphire substrate, which agrees with the XRD data. The pole figure of (001) plane shows three symmetric diffraction peaks split over 120° of rotational angle. From the pole figure of (020) plane of β-Ga_2O_3, six symmetric diffraction peaks were split over 60° of the rotation angle. Based on the Raman spectroscopy measurement from our previous studies,[26] the UID thin films grown on c-plane sapphire substrate were under a slight compressive strain. There was no obvious Raman peak shift for the Si-doped β-Ga_2O_3 thin films compared to those of the UID ones. This indicates that the level of doping achieved so far by LPCVD does not deteriorate the crystalline quality of the doped β-Ga_2O_3 thin films.

Optical properties of the as-grown thin films were characterized systematically. The room temperature absorbance spectrum of the Si-doped β-Ga_2O_3 thin film grown at 900 °C was shown in Fig. 4. The doped film has a carrier concentration of $\sim 1.4 \times 10^{19}\,cm^{-3}$. The thin film has a strong absorption in the deep UV region with a sharp absorption edge at around 260 nm. The estimated optical bandgaps obtained from the Tauc plot is $E_g \sim 4.76$ eV, as shown in the inset of Fig. 4. The above bandgap value is within the range of 4.5–4.9 eV for Ga_2O_3 thin films reported in the previous literatures.[39–41] However, it is worthwhile to mention here that the absorption edge does show a slight shift for films grown with different growth conditions or different doping levels. The room temperature PL and PLE spectra of the same doped β-Ga_2O_3 thin film were shown in Fig. 5. The room temperature PLE spectra were collected at the emission wavelengths of $\lambda_{emission} = 350$, 392, 420, 450, and 480 nm. The PLE spectrum collected with an emission wavelength of 450 nm had the strongest intensity. For all the emission wavelengths, the strong absorption occurred at around 260 nm. The PL spectra were measured with excitation wavelengths of $\lambda_{excitation} = 250$, 260, 270, 280, and 290 nm. Five distinct PL peaks appearing at 350, 392, 420, 450, and

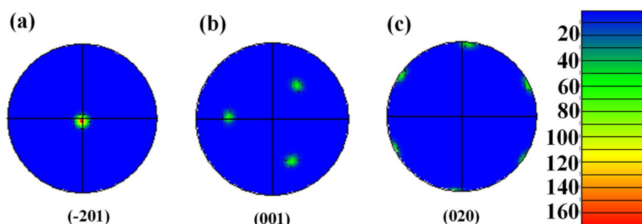

FIG. 3. Pole figures of UID β-Ga_2O_3 thin film grown on c-plane sapphire substrate: (a) (−201) plane, (b) (001) plane, and (c) (020) plane.

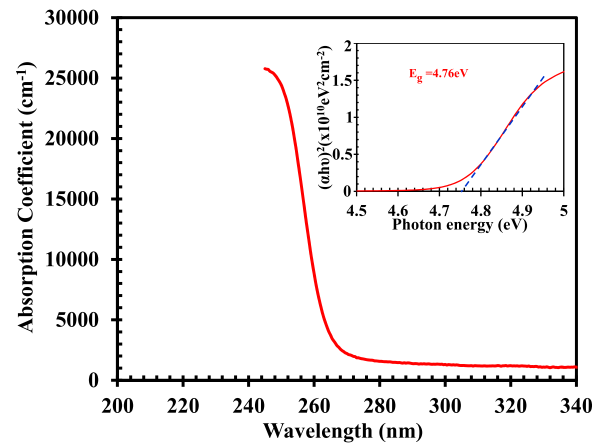

FIG. 4. Room temperature absorbance spectrum of Si-doped β-Ga_2O_3 thin film grown on c-plane sapphire substrate grown at 900 °C. The inset shows the Tauc plot of $(\alpha h\nu)^2$ versus photon energy ($h\nu$) for the thin film.

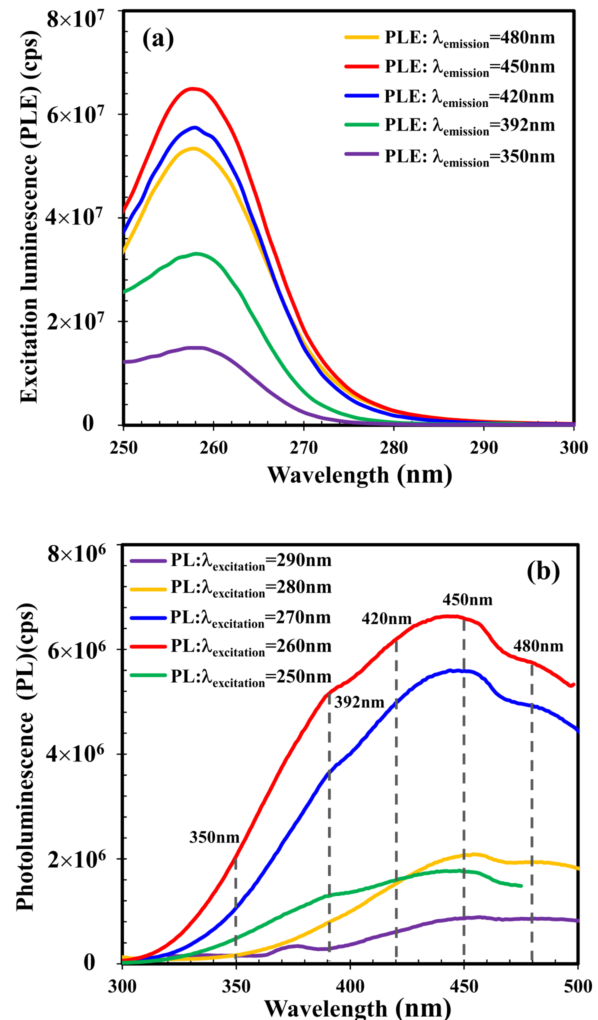

FIG. 5. Room temperature (a) excitation (PLE) and (b) photoluminescence (PL) spectrum of LPCVD grown Si-doped β-Ga_2O_3 thin film on c-plane sapphire substrate grown at 900 °C.

480 nm were observed. From our studies, the growth conditions affect significantly on the PL and PLE spectra of β-Ga_2O_3 films. The light-medium Si doping of β-Ga_2O_3 did not modify the PL or PLE spectra from that of the UID films. The PL spectra of the doped β-Ga_2O_3 thin film show a large Stokes shift, which may originate from the strong electron-phonon coupling caused by the localization of recombining electrons and holes. The UV emission at ~3.1 eV is an intrinsic emission and independent of growth conditions or dopants, which is attributed to the recombination of self-trapped excitons, as predicted from previous experimental studies[42–45] and first principle theoretical calculations.[46] As suggested from previous studies, the self-trapped excitons consisted of electrons on donors formed by oxygen vacancies $V_O{}^x$ and holes on acceptors formed by gallium vacancies $V_{Ga}{}^x$ or gallium-oxygen vacancy pairs (V_O–V_{Ga}). According to theoretical studies, the blue emission might originate from the recombination of a donor–acceptor pair (DAP) through tunneling.[43,45]

Hall measurements were carried out at room temperature on the as-grown β-Ga_2O_3 thin films using van der Pauw method. The applied magnetic field was 0.975 T. Figure 6(a) shows the dependence of n-type carrier concentration as a function of the Si precursor flow rate. The trend shows that the carrier concentration increases as the Si precursor flow rate increases. Figure 6(b) plots the Hall mobility as a function of the n-type carrier concentration for the as-grown Si-doped β-Ga_2O_3 thin films. By varying the doping source flow rate, the carrier concentration can be widely tuned between high-10^{16} to low-10^{19} cm^{-3} range. Among the selected growth conditions, the optimized electrical properties were exhibited by the film grown at 900 °C using an oxygen volume percentage of 4.8%. The measured room temperature Hall mobility was 42.35 cm^2/V s with an n-type carrier concentration of 1.32×10^{18} cm^{-3}, and the Hall resistivity was 1.11×10^{-1} Ω cm. The Hall measurement results indicate that Si is an effective n type dopant for β-Ga_2O_3 thin film, and the film electrical properties can be tuned by Si doping. The electrical properties of the LPCVD grown heteroepitaxial β-Ga_2O_3 thin films represent the best quality among the reported ones.

To better understand the electrical conduction mechanism of the Si doped β-Ga_2O_3 thin films, temperature dependent Hall measurements were performed. Figure 7 shows the temperature dependence of n type carrier concentration and the mobility of a Si doped β-Ga_2O_3 thin film having a carrier concentration of 3×10^{18} cm^{-3}. The activation energy of Si in β-Ga_2O_3 was estimated to be $E_a \sim 10.1$ meV ($n \sim e^{-\frac{E_a}{kT}}$) from the temperature dependence of the carrier concentration as shown in the inset of Figure 7. A peak mobility of ~41 cm^2/V·s was obtained at ~170 K, while the mobility decreases to 32 cm^2/V·s at room temperature. At low temperatures, the carrier concentration did not change substantially with temperature. This fact is because of conduction in an impurity band formed by donors in the bandgap. In highly doped semiconductors, neighboring donors' electron wavefunctions overlap and form a donor band. The electron motion takes place within this band by tunneling or hopping. At low temperatures, the conduction mechanism is dominated by donor band conduction. Thus the Hall carrier concentration increases weakly at low temperatures. Such dependence of Hall carrier concentration on temperature has been observed previously for highly doped β-Ga_2O_3 single crystals grown by EFG and floating zone methods.[47,48] In addition to the low mobility impurity band, the electron mobility is also limited by ionized impurity scattering at low temperatures and optical phonon scattering at high temperatures.[3,49]

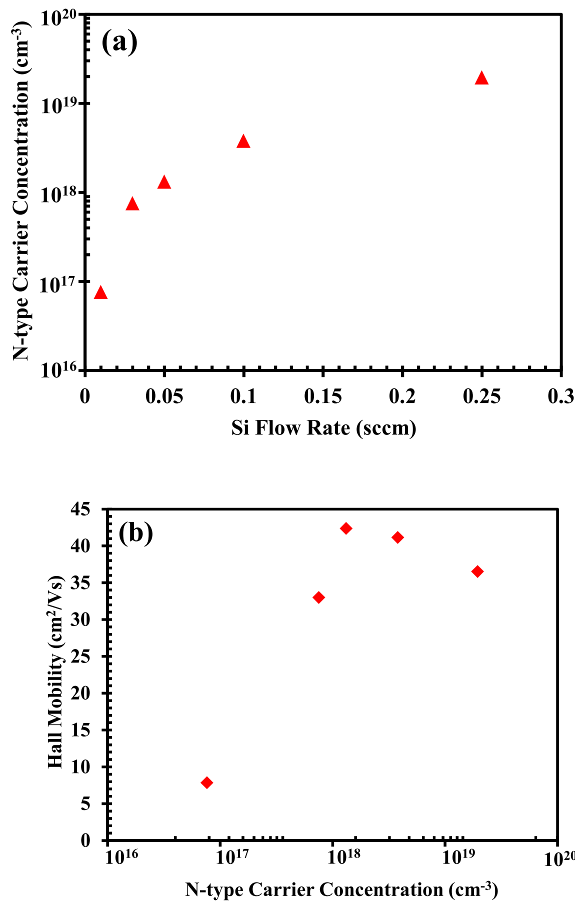

FIG. 6. (a) Relation between n-type carrier concentration and Si flow rate for the LPCVD grown Si-doped β-Ga_2O_3 thin film on c-plane sapphire substrate. (b) Electron Hall mobility as a function of carrier concentration for the LPCVD grown Si-doped β-Ga_2O_3 thin film on c-plane sapphire substrate.

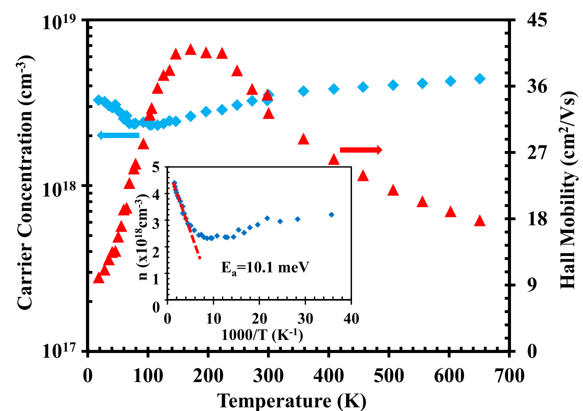

FIG. 7. Temperature dependent Hall measurement of carrier concentration and mobility for the LPCVD grown Si-doped β-Ga_2O_3 thin film on c-plane sapphire substrate. The inset shows the fitted line used for obtaining the activation energy for Si dopants.

The heteroepitaxy of β-Ga_2O_3 thin films on c-plane sapphire substrates by LPCVD was achieved with relatively high growth rates and good material quality. The relative broad FWHM of the (−201) XRD reflection peak indicates the existence of impurities and defects in the material. Additional material characterization is still required to better understand these defects and their origins. Further optimization of LPCVD growth of β-Ga_2O_3 films is expected to improve the material quality with better electrical property. Nevertheless, there is no previous report on the demonstration of effective n-type doping of a β-Ga_2O_3 thin film grown on foreign substrates. The promising results reveal the great potential to apply the heteroepitaxial β-Ga_2O_3 thin films for device applications.

In summary, the heteroepitaxial synthesis of n-type Si-doped β-Ga_2O_3 thin films on c-plane sapphire substrates by LPCVD was demonstrated. The crystal orientation and phase purity of β-Ga_2O_3 thin films on c-plane sapphire substrate were established by XRD and pole figure measurement. Effective n-type doping and doping control using Si for β-Ga_2O_3 heteroepitaxial thin films by LPCVD were achieved. Room temperature electron Hall mobility of 42.35 $cm^2/V\,s$ was measured for a Si-doped heteroepitaxial β-Ga_2O_3 film with a doping concentration of $1.32 \times 10^{18}\,cm^{-3}$. Advancements of LPCVD heteroepitaxy of UWBG β-Ga_2O_3 on sapphire substrates will open up opportunities for low cost high power electronic devices and solar blind deep-UV photodetectors.

We thank Dr. Nadeem Mahadik from the Naval Research Lab for his inputs on β-Ga_2O_3 XRD measurement. Part of the material characterization was performed at the Swagelok Center for Surface Analysis of Materials (SCSAM) at CWRU. S.M. and A.N. thank the funding support from the GHz-THz Electronics portfolio of the Air Force Office of Scientific Research (AFOSR).

[1]V. I. Nikolaev, A. I. Pechnikov, S. I. Stepanov, I. P. Nikitina, A. N. Smirnov, A. V. Chikiryaka, S. S. Sharofidinov, V. E. Bougrov, and A. E. Romanov, Mater. Sci. Semicond. Process. **47**, 16–19 (2016).
[2]H. Aida, K. Nishiguchi, H. Takeda, N. Aota, K. Sunakawa, and Y. Yaguchi, Jpn. J. Appl. Phys. **47**, 8506–8509 (2008).
[3]T. Oishi, Y. Koga, K. Harada, and M. Kasu, Appl. Phys. Express **8**, 031101 (2015).
[4]E. G. Villora, K. Shimamura, Y. Yoshikawa, K. Aoki, and N. Ichinose, J. Cryst. Growth **270**, 420–426 (2004).
[5]J. Zhang, B. Li, C. Xia, G. Pei, Q. Deng, Z. Yang, W. Xu, H. Shi, F. Wu, Y. Wu, and J. Xu, J. Phys. Chem. Solids **67**, 2448–2451 (2006).
[6]T. C. Lovejoy, E. N. Yitamben, N. Shamir, J. Morales, E. G. Villora, K. Shimamura, S. Zheng, F. S. Ohuchi, and M. A. Olmstead, Appl. Phys. Lett. **94**, 081906 (2009).
[7]Z. Galazka, R. Uecker, K. Irmscher, M. Albrecht, D. Klimm, M. Pietsch, M. Brutzam, R. Bertram, S. Ganschow, and R. Fornari, Cryst. Res. Technol. **45**, 1229–1236 (2010).
[8]K. Irmscher, Z. Galazka, M. Pietsch, R. Uecker, and R. Fornari, J. Appl. Phys. **110**, 063720 (2011).
[9]Z. Galazka, K. Irmscher, R. Uecker, R. Bertram, M. Pietsch, A. Kwasniewski, M. Naumann, T. Schulz, R. Schewski, D. Klimm, and M. Bickermann, J. Cryst. Growth **404**, 184–191 (2014).
[10]T. Oshima, N. Arai, N. Suzuki, S. Ohira, and S. Fujita, Thin Solid Films **516**, 5768–5771 (2008).
[11]K. Sasaki, A. Kuramata, T. Masui, E. G. Villora, K. Shimamura, and S. Yamakoshi, Appl. Phys. Express **5**, 035502 (2012).
[12]K. Sasaki, M. Higashiwaki, A. Kuramata, T. Masui, and S. Yamakoshi, J. Cryst. Growth **392**, 30–33 (2014).
[13]X. Du, W. Mi, C. Luan, Z. Li, C. Xia, and J. Ma, J. Cryst. Growth **404**, 75–79 (2014).
[14]G. Wagner, M. Baldini, D. Gogova, M. Schmidbauer, R. Schewski, M. Albrecht, Z. Galazka, D. Klimm, and R. Fornari, Phys. Status Solidi A **211**, 27–33 (2014).
[15]H. Murakami, K. Nomura, K. Goto, K. Sasaki, K. Kawara, Q. T. Thieu, R. Togashi, Y. Kumagai, M. Higashiwaki, and A. Kuramata, Appl. Phys. Express **8**, 015503 (2015).
[16]T. Oshima, T. Okuno, and S. Fujita, Jpn. J. Appl. Phys. **46**, 7217–7220 (2007).
[17]D. Guo, Z. Wu, P. Li, Y. An, H. Liu, X. Guo, H. Yan, G. Wang, C. Sun, L. Li, and W. Tang, Opt. Mater. Express **4**, 1067–1076 (2014).
[18]X. Z. Liu, P. Guo, T. Sheng, L. X. Qian, W. L. Zhang, and Y. R. Li, Opt. Mater. **51**, 203–207 (2016).
[19]V. Gottschalch, K. Mergenthaler, G. Wagner, J. Bauer, H. Paetzelt, C. Sturm, and U. Teschner, Phys. Status Solidi A **206**, 243–249 (2009).
[20]Y. Lv, J. Ma, W. Mi, C. Luan, Z. Zhu, and H. Xiao, Vacuum **86**, 1850–1854 (2012).
[21]W. Mi, J. Ma, Z. Zhu, C. Luan, Y. Lv, and H. Xiao, J. Cryst. Growth **354**, 93–97 (2012).
[22]N. M. Sbrockey, T. Salagaj, E. Coleman, G. S. Tompa, Y. Moon, and M. S. Kim, J. Electron. Mater. **44**, 1357 (2015).
[23]Y. Chen, H. Liang, X. Xia, P. Tao, R. Shen, Y. Liu, Y. Feng, Y. Zheng, X. Li, and G. Du, J. Mater. Sci.: Mater. Electron. **26**, 3231–3235 (2015).
[24]K. Kaneko, H. Ito, S.-D. Lee, and S. Fujita, Phys. Status Solidi C **10**, 1596–1599 (2013).
[25]T. Terasako, H. Ichinotani, and M. Yagi, Phys. Status Solidi C **12**, 985–988 (2015).
[26]S. Rafique, L. Han, and H. Zhao, Phys. Status Solidi A **213**, 1002–1009 (2016).
[27]S.-L. Ou, D.-S. Wuu, Y.-C. Fu, S.-P. Liu, R.-H. Horng, L. Liu, and Z.-C. Feng, Mater. Chem. Phys. **133**, 700–705 (2012).
[28]S. Muller, H. V. Wenckstern, D. Splith, F. Schmidt, and M. Grundmann, Phys. Status Solidi A **211**, 34–39 (2014).
[29]F. B. Zhang, K. Saito, T. Tanaka, M. Nishio, and Q. X. Guo, J. Cryst. Growth **387**, 96–100 (2014).
[30]Y. Wei, Y. Jinliang, W. Jiangyan, and Z. Liying, J. Semicond. **33**, 073003 (2012).
[31]K. H. Choi and H. C. Kang, Mater. Lett. **123**, 160–164 (2014).
[32]Z. Wu, G. Bai, Q. Hu, D. Guo, C. Sun, L. Ji, M. Lei, L. Li, P. Li, J. Hao, and W. Tang, Appl. Phys. Lett. **106**, 171910 (2015).
[33]S. Rafique, L. Han, M. J. Tadjer, J. A. Freitas, Jr., N. A. Mahadik, and H. Zhao, Appl. Phys. Lett. **108**, 182105 (2016).
[34]S. Rafique, L. Han, C. A. Zorman, and H. Zhao, Cryst. Growth Des. **16**, 511–517 (2016).
[35]E. G. Villora, K. Shimamura, Y. Yoshikawa, T. Ujiie, and K. Aoki, Appl. Phys. Lett. **92**, 202120 (2008).
[36]D. Gogova, G. Wagner, M. Baldini, M. Schmidbauer, K. Irmscher, R. Schewski, and Z. Galazka, J. Cryst. Growth **401**, 665–669 (2014).
[37]S. Nakagomi and Y. Kokubun, J. Cryst. Growth **349**, 12–18 (2012).
[38]M. A. Tadjer, M. A. Mastro, N. A. Mahadik, M. Currie, V. D. Wheeler, J. A. Freitas, Jr., J. D. Greenlee, J. K. Hite, K. D. Hobart, C. R. Eddy, Jr., and F. J. Kub, J. Electron. Mater. **45**, 2031 (2016).
[39]E. G. Villora, M. Yamaga, T. Inoue, S. Yabasi, Y. Masui, T. Sugawara, and T. Fukuda, Jpn. J. Appl. Phys. **41**, L622–L625 (2002).
[40]H. H. Tippins, Phys. Rev. **140**, A316 (1965).
[41]K. Shimamura, E. G. Villora, T. Ujjie, and K. Aoki, Appl. Phys. Lett. **92**, 201914 (2008).
[42]B. C. Kim, K. T. Sun, K. S. Park, K. J. Im, T. Noh, M. Y. Sung, S. Kim, S. Nahm, Y. N. Choi, and S. S. Park, Appl. Phys. Lett. **80**, 479 (2002).
[43]L. Binet and D. Gourier, J. Phys. Chem. Solids **59**, 1241–1249 (1998).
[44]J. B. Varley, J. R. Weber, A. Janotti, and C. G. Van De Walle, Appl. Phys. Lett. **97**, 142106 (2010).
[45]T. Harwig and F. Kellendonk, J. Solid State Chem. **24**, 255–263 (1978).
[46]J. B. Varley, A. Janotti, C. Franchini, and C. G. Van de Walle, Phys. Rev. B **85**, 081109 (2012).
[47]T. Oishi, K. Harada, Y. Koga, and M. Kasu, Jpn. J. Appl. Phys. **55**, 030305 (2016).
[48]E. G. Villora, K. Shimamaura, T. Ujiie, and K. Aoki, Appl. Phys. Lett. **92**, 202118 (2008).
[49]M. J. Tadjer, N. A. Mahadik, V. D. Wheeler, E. R. Glaser, L. Ruppalt, A. D. Koehler, K. D. Hobart, C. R. Eddy, Jr., and F. J. Kub, ECS J. Solid State Sci. Technol. **5**, P468–P470 (2016).